Protein Profiling of Rat Ventral Prostate following Chronic Finasteride Administration

IDENTIFICATION AND LOCALIZATION OF A NOVEL PUTATIVE ANDROGEN-REGULATED PROTEIN*[S]

Corinne Cayatte‡§¶, Catherine Pons‡, Jean-Marie Guigonis‖, Jérôme Pizzol‡, Laetitia Elies§, Philippe Kennel§, David Rouquié§, Rémi Bars§, Bernard Rossi‡, and Michel Samson‡**

To better understand the effects of antiandrogens on the prostate, we investigated the changes in the proteome of rat ventral prostate (VP) following treatment with a well characterized 5α-reductase inhibitor, finasteride. Sprague-Dawley rats were treated daily by gavage with finasteride at 0, 1, 5, 25, and 125 mg/kg/day. Changes in plasma hormone levels as well as the weight and histology of sex accessory tissues were determined after 28 days of treatment and showed a dose-related decrease of VP weights together with a marked atrophy of the tissue visible at the macroscopic and microscopic levels. In addition, significant reductions in seminal vesicle and epididymis weights were noted. VP proteins were analyzed by two-dimensional gel electrophoresis: 37 proteins, mainly involved in protein synthesis, processing, and cellular trafficking and in metabolism, detoxification, and oxidative stress, were identified as modulated by finasteride. The prominent feature of this study is the demonstration of finasteride dose-dependent up-regulation of a protein similar to L-amino-acid oxidase 1 (Lao1). An up-regulation of this protein was also observed with the antiandrogen flutamide. Lao1 expression occurred as early as 48 h after antiandrogen administration and persisted throughout the treatment duration. Immunohistochemistry showed that this protein was only detectable in epithelial cells and secretory vesicles. Altogether these data point to a potential use of Lao1 to reveal antiandrogen-induced prostate injury. ***Molecular & Cellular Proteomics 5:2031–2043, 2006.***

Prostate growth and homeostasis are controlled by androgens through their interaction with the nuclear androgen receptor (AR).[1] This intranuclear receptor acts as a DNA-binding transcription factor, which regulates the expression of an array of target genes (1). Castration of young adult rats causes a reduction in testosterone, which induces a dramatic regression of prostate cell number as well as the secretory activity of the prostate (2). Such tissue damage can also be chemically induced by therapeutic drugs or by some environmental pollutants that exhibit antiandrogenic activity (3). Due to the widespread use of man-made chemicals, the identification of those that potentially interfere with reproductive functions has become a real public health issue. These so-called endocrine disruptors are thought to be responsible for sperm infertility in adult men (4) and for impairments of sex organ development during puberty in individuals that have been exposed to the chemical *in utero* (5).

Finasteride, a drug widely used in the treatment of alopecia and benign prostatic hyperplasia (6), acts on rat prostate through inhibition of the 5α-reductase (5αR) (7, 8), an enzyme that converts testosterone into the more potent androgen dihydrotestosterone (DHT). Both short (15 days) and long term (1–2 years) exposure of rats to this compound have already been shown to induce a marked decrease in intraprostatic DHT levels that is followed by a reduction of the ventral lobe weight. Moreover morphometric analyses revealed a significant decrease in absolute volume of both glandular epithelial and stromal compartments of rat prostate with a subsequent reduction in prostate secretions (9–11). It has also been demonstrated that rat prostate involution observed under finasteride treatment is partly due to apoptosis (11) and to a dramatic regression of prostate vascularization (12).

The 28-day toxicity study in the rat and its recent enhancement of the test guideline 407 designed by the Organisation for Economic Co-operation and Development (OECD guideline for testing of chemicals; adopted by the council on July, 27 1995; Repeated Dose 28-day Oral Toxicity Study in Rodents) (13, 14) has recently been proposed for the detection of endocrine-mediated effects from chemicals such as finasteride. Thus, the following study based on the OECD 28-day

From the ‡INSERM U638, ‖Institut Fédératif de Recherche 50, Faculté de Médecine, avenue de Valombrose, 06107 Nice cedex 02, France and §Bayer CropScience, 355 rue Dostoïevski, 06903 Sophia-Antipolis, France

Received, May 3, 2006, and in revised form, June 23, 2006
Published, MCP Papers in Press, July 12, 2006, DOI 10.1074/mcp.M600165-MCP200

[1] The abbreviations used are: AR, androgen receptor; 2D-gel, two-dimensional gel electrophoresis; DHT, dihydrotestosterone; HSP, heat shock protein; Lao1, L-amino-acid oxidases; LH, luteinizing hormone; RH, rehydration buffer; T_3, triiodothyronine; T_4, thyroxine; T, testosterone; TSH, thyroid-stimulating hormone; VP, ventral prostate; 5αR, 5α-reductase; ANOVA, analysis of variance; GAPDH, glyceraldehyde-3-phosphate dehydrogenase; COP, coatomer protein.

studies was designed to investigate the molecular events associated with the atrophy of VP induced by a chronic exposure to the 5αR inhibitor finasteride. Although the effects of androgen deprivation on prostate morphology and physiology are well documented, the underlying molecular mechanisms remain unclear. Many recent studies have attempted to explain these processes through transcriptome analyses (15–17). However, as there are growing evidences that an increase at the transcriptional level is not necessarily correlated with an increase of the encoded protein (18), we decided to include a proteomics component to our study.

Under our experimental conditions, finasteride induced ventral prostate weight loss and atrophy and modified the expression level of 37 proteins as revealed by two-dimensional gel electrophoresis (2D-gel) pattern analyses. These analyses highlighted a dose-dependent up-regulation of a protein similar to Lao1 that is specifically expressed by prostate epithelial cells. Under treatment with an antiandrogen (flutamide) (19), we confirmed that a dose-dependent high level of expression of Lao1 was achieved at early time points (48 h) and persisted after 28 days of treatment. Because of the production of H_2O_2 by Lao1 it is conceivable that the resulting oxidative stress may contribute to the deleterious effect of the antiandrogens.

EXPERIMENTAL PROCEDURES

Toxicology Study

Chemicals and Dose Preparations

Finasteride (Chemical Abstracts Service number 98319-26-7, APIN Chemicals Ltd., Oxfordshire, UK) and flutamide (Chemical Abstracts Service number 13311-84-7, Sigma) were stored in an air-tight, light-resistant container at room temperature. The dosing formulations of finasteride and flutamide were prepared at the required concentrations in aqueous 0.5% (w/v) methylcellulose weekly and every other week, respectively, and stored at 4 °C.

Animals

All animal work was performed at Bayer CropScience (Sophia-Antipolis, France) in accordance to the French laws for animal experimentation. The protocol, in-life phase, raw data, and study report were performed according to standard operating procedures that were previously accepted and periodically inspected by a Quality Assurance Unit.

Male Sprague-Dawley rats (Ico: OFA-SD (Specific Pathogen-Free Caw)) were obtained from Charles River Laboratories (L'Arbresle, France). Animals were 6–7 weeks old at the start of the experiment and were housed individually. Certified rodent pelleted and irradiated diet (reference A04C-10, Scientific Animal Food and Engineering, Epinay-sur-Orge, France) and filtered tap water were available *ad libitum*.

Experimental Designs

Long Term Treatment—Groups of six rats per experimental condition were constituted using a computerized randomization procedure that ensures a similar body weight distribution among groups. The animals received by gavage a single daily dose of either the vehicle alone (0.5% aqueous methylcellulose) as control or the test substances for 28 days. Based on previous data generated at Bayer CropScience Sophia-Antipolis,[2] the dose levels were selected as follows: finasteride was given at 1, 5, 25, or 125 mg/kg/day, and flutamide was given at 6, 30, or 150 mg/kg/day. A dosing volume of 5 ml/kg of body weight was used for the duration of the study and adjusted at weekly intervals according to individual body weights.

Short Term Treatment—After an overnight fast, randomized groups of six rats per experimental condition were given by gavage a single bolus of the vehicle alone (0.5% aqueous methylcellulose) as control or flutamide at a dose level of 150 mg/kg using a dosing volume of 5 ml/kg of body weight.

Animal Euthanasia—All animals were sacrificed in a randomized fashion by exsanguination under deep anesthesia (pentobarbital, intraperitoneal injection of 60 mg/kg of body weight) between 8:00 a.m. and 12:00 a.m. either 24 or 48 h after dosing (short term treatment) or 24 h after the last dose (day 29, long term treatment).

Hormone Analysis

At sacrifice, blood samples from the abdominal aorta were collected in lithium heparin-containing tubes, and the resulting plasma samples were kept frozen (−20 °C) until the determination of triiodothyronine (T_3), thyronine (T_4), thyroid-stimulating hormone (TSH), luteinizing hormone (LH), and testosterone (T) levels could be performed using specific radioimmunoassay kits (Amersham Biosciences for TSH and LH and Beckman Coulter, Villepinte, Paris, France for T_3, T_4, and T).

Postmortem Examination and Organ Weights

The following organs were collected and weighed: brain, kidney, liver, dorsolateral and ventral prostate, testes (individually), thyroid gland (with parathyroid gland), penis glans, seminal vesicles (with coagulating gland), adrenal gland, Cowper gland, levator ani and bulbocavernosus muscles, and epididymides (individually). VP was halved: one half was preserved in 10% neutral buffered formalin for histological analysis, and the other half was weighed, snap frozen in liquid nitrogen, and stored frozen below −70 °C until proteome analysis.

Statistical Analyses

Statistical analyses on body and organ weights and hormonal parameters were calculated for each group, and Bartlett's test was performed to compare the homogeneity of group variances. If Bartlett's test was not significant ($\alpha = 5\%$), means were compared using the analysis of variance (ANOVA). If the ANOVA was significant ($\alpha = 5\%$), means of the exposed groups were compared with the mean of the control group using Dunnett's test.

For body and organ weights, if Bartlett's test was significant ($\alpha = 5\%$), group means were compared using the non-parametric Kruskal-Wallis test. If the latter was not significant, the group means were considered to be homogeneous, and no further analysis was performed. If the Kruskal-Wallis test was significant ($\alpha = 5\%$), means of the exposed groups were compared with the mean of the control group using Dunn's test.

For the hormonal parameters, if Bartlett's test was significant ($\alpha = 5\%$), data were transformed using the log transformation. If Bartlett's test on log-transformed data was not significant, means were compared using the ANOVA on log-transformed data. If the ANOVA on log-transformed data was not significant ($\alpha = 5\%$), the group means were considered homogeneous, and no further analysis was performed. If the ANOVA on log-transformed data was significant ($\alpha =$

[2] P. Kennel and R. Bars, unpublished data.

5%), means of the exposed groups were compared with the mean of the control group using Dunnett's test on log-transformed data. If Bartlett's test on log-transformed data was significant, group means were compared using the non-parametric Kruskal-Wallis test. If the latter was not significant, the group means were considered to be homogeneous, and no further analysis was performed. If the Kruskal-Wallis test was significant ($\alpha = 5\%$), means of the exposed groups were compared with the mean of the control group using Dunn's test.

All the statistical tests were two-sided tests. Group means were compared at α level 5 and 1%. Statistical analyses were performed using the software PathTox System Version 4.2.2 (Xybion Corp., Cedar Knolls, NJ).

Histopathology

Formalin-fixed VP samples were embedded in paraffin wax. Histological sections (5 μm) were stained with eosin and hematoxylin for microscopic examination.

Immunohistochemistry

Histological sections (5 μm) were immunohistochemically stained using antibodies against Ki-67 (reference 550609, BD Pharmingen) according to the manufacturer's instructions and using an autostainer, Discovery XT system (Ventana Medical Systems, Illkirch, France). Cell counting was done using Morpho Expert (Explora Nova, La Rochelle, France), and at least 1000 epithelial cells were counted for each control and each treated animal (finasteride, 125 mg/kg/day). The indices of Ki-67-positive cells are expressed as a percentage of the total number of cells counted. Data statistical analysis was performed using Pearson's χ^2 test with Yates' continuity correction.

Localization of Lao1 expression was investigated on 5-μm sections of VP of control and finasteride-treated rats (25 mg/kg/day) stained according to the manufacturer's protocol number 38 (autostainer Discovery XT system, Ventana Medical Systems) with an anti-Lao antibody (Nordic Immunological Laboratories, Tilburg, The Netherlands) incubated for 60 min at 20 μg/ml.

Proteome Analysis

Sample Preparation

Frozen VPs were homogenized in rehydration buffer (RH) containing 7 M urea, 2 M thiourea, 4% CHAPS (electrophoretic grade, Sigma) using a Dounce homogenizer followed by a Tenbroeck homogenizer. After centrifugation (30 min, 22,000 $\times$ *g*, 15 °C), the protein concentration was determined in the supernatant by the Bradford assay (Bio-Rad) using bovine serum albumin in RH as a standard curve. The pellet containing RH-insoluble material was resuspended in 10 mM Na_2HPO_4, 10% glycerol (v/v), 3% SDS (w/v); sonicated (7 min, 400 watts, Deltasonic, Meaux, France); and centrifuged (30 min, 22,000 $\times$ *g*, room temperature). The protein concentration of the supernatant was determined using DC™ protein assay (Bio-Rad). Both extracts were kept frozen at −80 °C until used.

One-dimensional Gel Electrophoresis

Proteins solubilized in RH were adjusted to 3% SDS (w/v), supplemented with 5% β-mercaptoethanol (v/v), and 0.05% bromphenol blue (w/v) and incubated at 37 °C for 10 min prior to electrophoresis. RH-insoluble material in SDS-containing buffer was supplemented with 5% β-mercaptoethanol (v/v) and 0.05% bromphenol blue (w/v) and boiled for 5 min. SDS-PAGE was performed according to Laemmli (20): proteins (75 μg/lane) were separated on 1.5-mm-thick slab gels using a 3% acrylamide stacking gel and a 5–15% acrylamide linear gradient as resolving gel. Gels were run overnight at constant current (8 mA/gel). Proteins were then transferred on PVDF membrane as described below.

Two-dimensional Gel Electrophoresis and Protein Staining

Using a cup-loading system (Bio-Rad), 500 μg of each lysate were supplemented with 100 mM 2-hydroxyethyl disulfide (reference 373890250, Acros Organics, Geel, Belgium) (21). The samples were loaded onto IPG ReadyStrips™ pH 3–10, pH 3–6, pH 5–8, or pH 7–10 (17 cm, linear gradient, Bio-Rad) and rehydrated with 300 μl of RH supplemented with 100 mM 2-hydroxyethyl disulfide (8 h of passive rehydration at 20 °C). Isoelectric focusing on the Protean IEF cell from Bio-Rad was carried out as follows: 15 min at 250 V, a slow (15-h) voltage ramping to 10,000 V, and a final step at 10,000 V up to 300,000 V-h. Immediately after focusing, IPG strips were wrapped in plastic trays (rehydration trays, Bio-Rad) and stored at −80 °C. Prior to SDS-PAGE, proteins in the IPG were reduced with 130 mM DTT solubilized in 1.5 M Tris, pH 8.8, containing 4% SDS and 30% glycerol for 15 min and alkylated with 130 mM iodoacetamide solubilized in 1.5 M Tris, pH 8.8, containing 4% SDS and 30% glycerol for 20 min, and finally strips were equilibrated in 4% SDS, 30% glycerol, 1 M Tris, pH 6.8, for 60 min. The second dimension separation was run overnight at room temperature on a 1-mm-thick 10% polyacrylamide gel at a constant voltage up to 1300 V-h (Protean II XL cell). Immediately after electrophoresis, gels were fixed in 40% ethanol, 3% phosphoric acid for 2 h, rinsed with deionized water three times for 30 min, and then stained for 16 h with Bio-Safe Coomassie stain (Bio-Rad). Gels were scanned using a GS-800 calibrated densitometer (Bio-Rad).

Protein patterns were compared using PD-Quest imaging system (Version 7.1, Bio-Rad): expression levels of the proteins were quantified by analyzing the intensity of each spot. After normalization (based on total quantity of valid spots on the gels), statistical differences in expression between control and treated animals were assessed through the Mann-Whitney test. Spots with a p value ≤ 0.05 were considered to be statistically significant and were subsequently treated for identification by mass spectrometry.

In-gel Tryptic Digestion and Protein Identification by Mass Spectrometry

The protein spots of interest were manually excised from the 2D-gel and destained with 50% acetonitrile in 25 mM ammonium bicarbonate. Gel pieces were crushed in an Eppendorf tube, dehydrated with acetonitrile for 5 min, and vacuum-dried. Gel pieces were then rehydrated with 15 μl of 25 mM ammonium bicarbonate, 10% acetonitrile supplemented with trypsin (5 ng/μl, reference V5111, Promega, Madison, WI) at 37 °C for 16 h. Afterward tryptic peptides were extracted by 15-min incubations consecutively in 5% formic acid, 50% acetonitrile, and 80% acetonitrile. Sonications (7 min, 400 watts, Deltasonic) were also performed during incubations to facilitate peptide extraction. Extracts were pooled before being evaporated under vacuum, and dry peptide samples were redissolved in 5% formic acid, 20% methanol.

Mass spectra were recorded with a MALDI-TOF spectrometer (Voyager DE-PRO, PerSeptive Biosystems, Framingham, MA) set in positive reflectron mode. Samples were spotted on a thin layer of nitrocellulose (0.5 μl of a 5 mg/ml solution in acetone/isopropanol/acetic acid (1:1:2, v/v/v)) and then overlaid with α-cyano-4-hydroxycinnamic acid (0.75 μl of a 10 mg/ml solution in 50% acetonitrile, 0.3% TFA). The TOF was measured using the following parameters: 20-kV accelerating voltage, 74% grid voltage, 0.002% guide wire voltage, 250-ns delay time, and 500 low mass gate. External calibration was performed using angiotensin 1 ($M + H^+$, 1296.68), adrenocorticotropic hormone (clip 18–39, $M + H^+$, 2465.19; and clip 7–38, $M + H^+$, 3657.93) in the same series as the sample to analyze.

TABLE I

Effects of finasteride on body weight and sex organ and accessory tissue weights

Bold characters refer to values statistically different from control. Values in parentheses refer to the percentage of weight loss compared with control.

	Control	Finasteride (mg/kg/day)			
		1	5	25	125
Body weight (g) at terminal sacrifice	387 ± 18	383 ± 30 (−1%)	378 ± 8 (−2%)	379 ± 30 (−2%)	365 ± 20 (−6%)
Organ weight (g) (mean ± S.D.)					
Ventral prostate	0.46 ± 0.12	0.27 ± 0.09 (−41%)	0.23 ± 0.06 (−50%)	**0.21 ± 0.04 (−54%)[a]**	**0.15 ± 0.03 (−67%)[b]**
Dorsal prostate	0.14 ± 0.07	0.11 ± 0.05 (−21%)	0.09 ± 0.03 (−36%)	0.09 ± 0.03 (−36%)	0.07 ± 0.03 (−50%)
Seminal vesicles	1.24 ± 0.41	0.73 ± 0.24 (−41%)	0.63 ± 0.06 (−49%)	**0.53 ± 0.18 (−57%)[a]**	**0.36 ± 0.17 (−71%)[b]**
Cowper glands	0.08 ± 0.01	**0.056 ± 0.01 (−30%)[a]**	0.06 ± 0.01 (−20%)	**0.04 ± 0.01 (−46%)[b]**	**0.03 ± 0.01 (−61%)[b]**
Right epididymis	0.50 ± 0.06	0.48 ± 0.07 (−4%)	0.45 ± 0.04 (−10%)	**0.39 ± 0.09 (−22%)[a]**	**0.37 ± 0.03 (−26%)[a]**
Left epididymis	0.48 ± 0.05	0.46 ± 0.05 (−4%)	0.46 ± 0.05 (−4%)	0.39 ± 0.08 (−19%)	0.39 ± 0.05 (−19%)
LABC[c] muscle	0.70 ± 0.08	0.64 ± 0.08 (−9%)	0.66 ± 0.09 (−7%)	0.6 ± 0.07 (−14%)	0.58 ± 0.12 (−17%)

[a] $p < 0.05$; $n = 6$.
[b] $p < 0.01$; $n = 6$.
[c] LABC, levator ani and bulbocavernosus.

Internal calibration was also performed using autodigestion peaks of trypsin ($M + H^+$, 515.33, 842.51, 1045.56, and 2211.10). Peptide mass profiles obtained by MALDI-MS were analyzed using Protein Prospector (version 3.2.1) software. Peptide masses were compared with the theoretical masses derived from the sequences contained in Swiss-Prot/TrEMBL databases or deduced from the non-redundant National Center for Biotechnology Information (nrNCBI) database. The search parameters were set as follows: cysteines as carbamidomethyl derivative; allowed peptide mass error, 50–100 ppm; at least four peptide mass hits required for protein match; up to one missed cleavage; and methionine-oxidized form. Restrictions were placed neither on species of origin, pI, nor protein mass range.

To confirm peptide mass fingerprinting results, some samples were analyzed by nano-ESI-MS/MS (static infusion) on an LCQ^{DECA} XP-PLUS mass spectrometer (ThermoQuest, San Jose, CA). Nanoelectrospray capillaries (ES 381, PROXEON Biosystems, Odense, Denmark) were used as emitter. The parameters for nano-ESI were set as follows: voltage, 1 kV; current, 0.15 μA; capillary voltage, 35 V; capillary temperature, 175 °C; auxiliary/sweep flow rate, 10. For MS/MS, CID was set at 35–40 V. Each MS/MS spectrum was optimized to obtain the best signal/noise ratio. No smoothing was applied. Q activation was set at 0.220 to cover the largest mass range in MS/MS. The quasimolecular ion detected in MS (full scan) was analyzed by MS/MS with an isolation width (*m/z*) set between 2 and 3 to improve the resolution for *de novo* sequencing. Acquired MS/MS spectra were interpreted using Bioworks (version 3.1 ThermoQuest) and MASCOT (on line) or DeNovoX (Version 1.0, ThermoQuest) softwares. Both b and y ion series were used to search against Swiss-Prot/TrEMBL or nrNCBI databases without restriction of charge state and a threshold set at 10^4. The search level was restricted to MS^2 spectra. None of the identified doubly charged ions (the charge was determined from zoom scan data) had an Xcorr below 2.

Only data from MS/MS spectra with an intensity $>10^5$ were used for *de novo* sequencing analyses performed with DeNovoX software with the following settings: match tolerance from 0.5 to 0.7 Da, peak integration, and noise filter selected with a filter scope set at the default value 200.

Western Blotting

Protein extracts of rat VP, separated by one- or two-dimensional gel electrophoresis, were transferred in Tris-HCl methanol (20 mM Tris, 150 mM glycine, 20% methanol) (500 mA, 4 h, 4 °C) onto PVDF membranes (Millipore Corp., Bedford MA). Immediately after transfer, membranes were soaked in Amido Black (0.1% naphthol blue black, 10% methanol, 2% acetic acid); washed in 50% methanol, 7% acetic acid; and scanned. They were then incubated for 2 h at room temperature with blocking buffer TBST (150 mM NaCl, 10 mM Tris-HCl, 0.01% Tween 20, pH 7.5) containing 5% (w/v) nonfat dry milk. Membranes were then incubated overnight at 4 °C with either anti-Lao antibodies (2 μg/ml, Nordic Immunological Laboratories) or anti-phosphotyrosine (1 μg/ml, clone 4G10, Upstate Biotechnology, Lake Placid, NY). After three washes for 10 min with TBST, the membranes were incubated for 1 h at room temperature with anti-rabbit immunoglobulin goat polyclonal antibodies (reference P0448, Dako, Glostrup, Denmark) or anti-mouse immunoglobulin goat polyclonal antibodies (Dako reference P0447) conjugated to horseradish peroxidase both used at a 1:5000 dilution in TBST. They were then washed three times for 10 min in TBST and finally incubated for 1 min with ECL™ (Amersham Biosciences). Detection was performed with autoradiography films (BioMax Light film, Eastman Kodak Co.). Total band intensities per lane were assessed using NIH Image (Version 1.62) software.

RESULTS

Finasteride, a model compound for DHT withdrawal, was administered daily by gavage to young adult male Sprague-Dawley rats at different dose levels (0, 1, 5, 25, and 125 mg/kg/day). After 28 days of treatment, hormone levels (LH, TSH, T_3, T_4, and T) were measured on blood samples, and reproductive tissues including VP were removed, weighed, and examined microscopically.

Effects of Finasteride on Body Weight and Sex Organ Weight—Treatment with finasteride did not induce any mortalities or clinical signs. No effect on food consumption was observed at any dose level (data not shown). A slight decrease in body weight gain was noted at 125 mg/kg/day (−11%, not statistically significant) when compared with the control group (Table I). Overall there was a dose-related decrease in most of the sex organ and accessory tissue weights, the difference being statistically significant at 25 and 125 mg/kg/day for VP, seminal vesicles, Cowper gland, and right

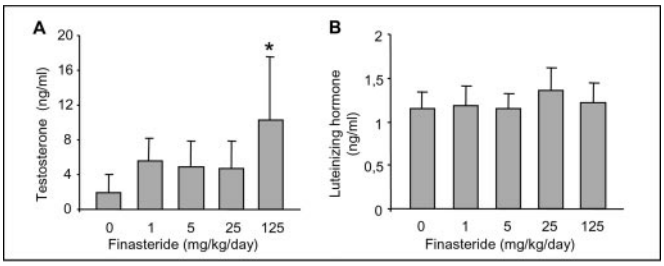

FIG. 1. **Effects of finasteride on testosterone and luteinizing hormone circulating levels.** *A*, each *bar* represents the mean value ± S.D. of six animals per group. *, statistically different from testosterone control value ($p < 0.05$). *B*, each *bar* represents the mean value ± S.D. of at least four animals per group.

epididymis (Table I). Ventral prostate weights decreased by 54% ($p < 0.05$) and 67% ($p < 0.01$) at finasteride doses of 25 and 125 mg/kg/day, respectively. No effects were observed on the weight of other tissues.

Effects of Finasteride on Hormone Levels—At sacrifice, mean T circulating concentration was found to be markedly increased only at the highest dose of finasteride (+435%, $p < 0.05$) (Fig. 1*A*). No apparent differences between control and treated animals were observed for LH (Fig. 1*B*), T_3, T_4, or TSH levels (data not shown).

Effects of Finasteride on Ventral Prostate Morphology and Epithelial Cell Proliferation—VPs from control and treated rats were fixed, sectioned, stained, and examined microscopically. Histological examination revealed atrophy of VP mainly characterized by a general reduction in size without prominent morphological changes; albeit some epithelium shrinkage could be observed in glandular ducts at the highest dose of finasteride. The number of animals that exhibited atrophy of the VP increased with increasing concentration of finasteride administered (Fig. 2, *A* and *B*). To evaluate finasteride effects on epithelial cell proliferation, VP sections of control and treated rats (125 mg/kg/day) were stained with an antibody raised against Ki-67, a nuclear cell proliferation-associated antigen expressed in all active stages of the cell cycle. Ki-67-positive cell indices revealed a statistically significant ($p < 0.001$) decrease of cell proliferation in treated rats (Fig. 2, *C* and *D*).

Proteome Analysis of Ventral Prostates of Control and Treated Animals—In an attempt to elucidate the processes leading to prostate atrophy and subsequent weight loss, proteome analysis was undertaken. Proteins extracted from the VPs of control and all finasteride-treated animals were separated by 2D-gel and stained with the mass spectrometry-compatible colloidal Coomassie Blue (22). This powerful technique (23) allowed the separation and detection of approximately 1000 spots per organ, distributed over the different pH gradients used in this study.

Representative Coomassie Blue-stained gels of VP proteins from control and finasteride (1 mg/kg/day)-treated rats are depicted in Fig. 3. Spots modulated by finasteride treatment

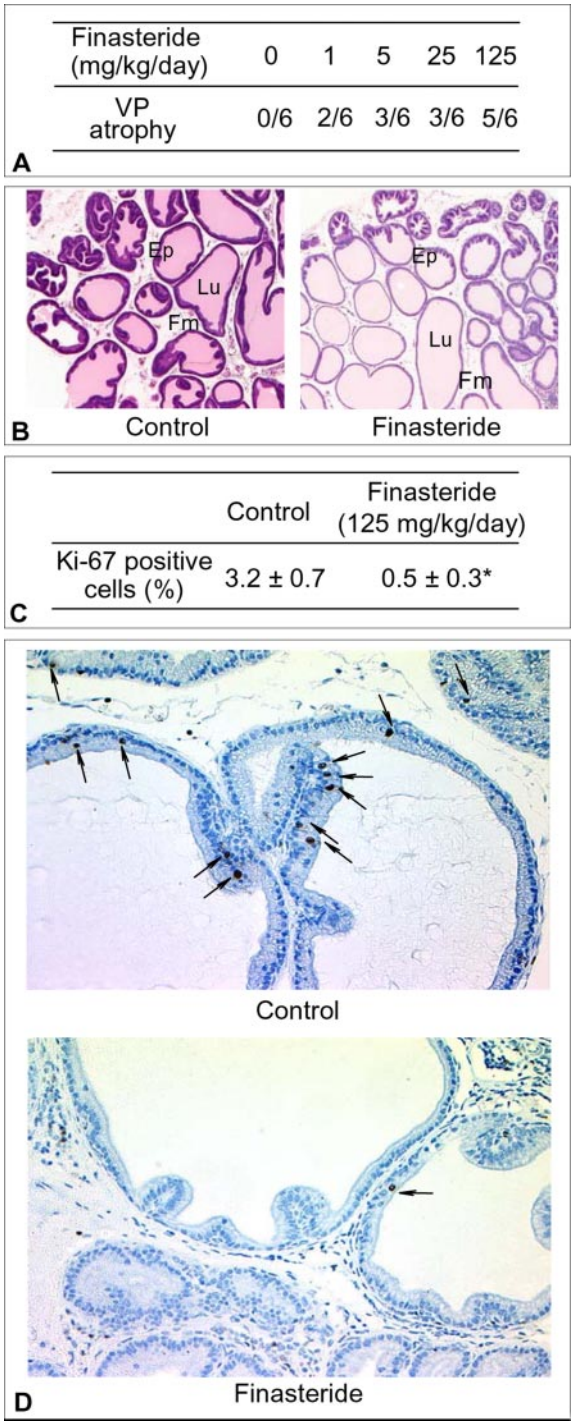

FIG. 2. **Effects of finasteride on ventral prostate morphology and epithelial cell proliferation.** *A*, incidence of ventral prostate atrophy: the morphology of these tissues was normal, but their size was reduced. *B*, ventral prostate sections from control and treated rat (125 mg/kg/day) stained with eosin and hematoxylin. *Magnification*, 50×. *Lu*, lumen; *Ep*, glandular epithelial cells; *Fm*, fibromuscular stroma cells. *C*, mean ± S.D. of Ki-67-positive cell indices (%) in VP epithelial compartment of six control and six treated animals (125 mg/kg/day). *, statistically different from control value ($p < 0.001$). *D*, immunostaining of Ki-67-positive cells on VP sections of control and treated rats (125 mg/kg/day). *Arrows* indicate Ki-67-positive cells. *Magnification*, ×200.

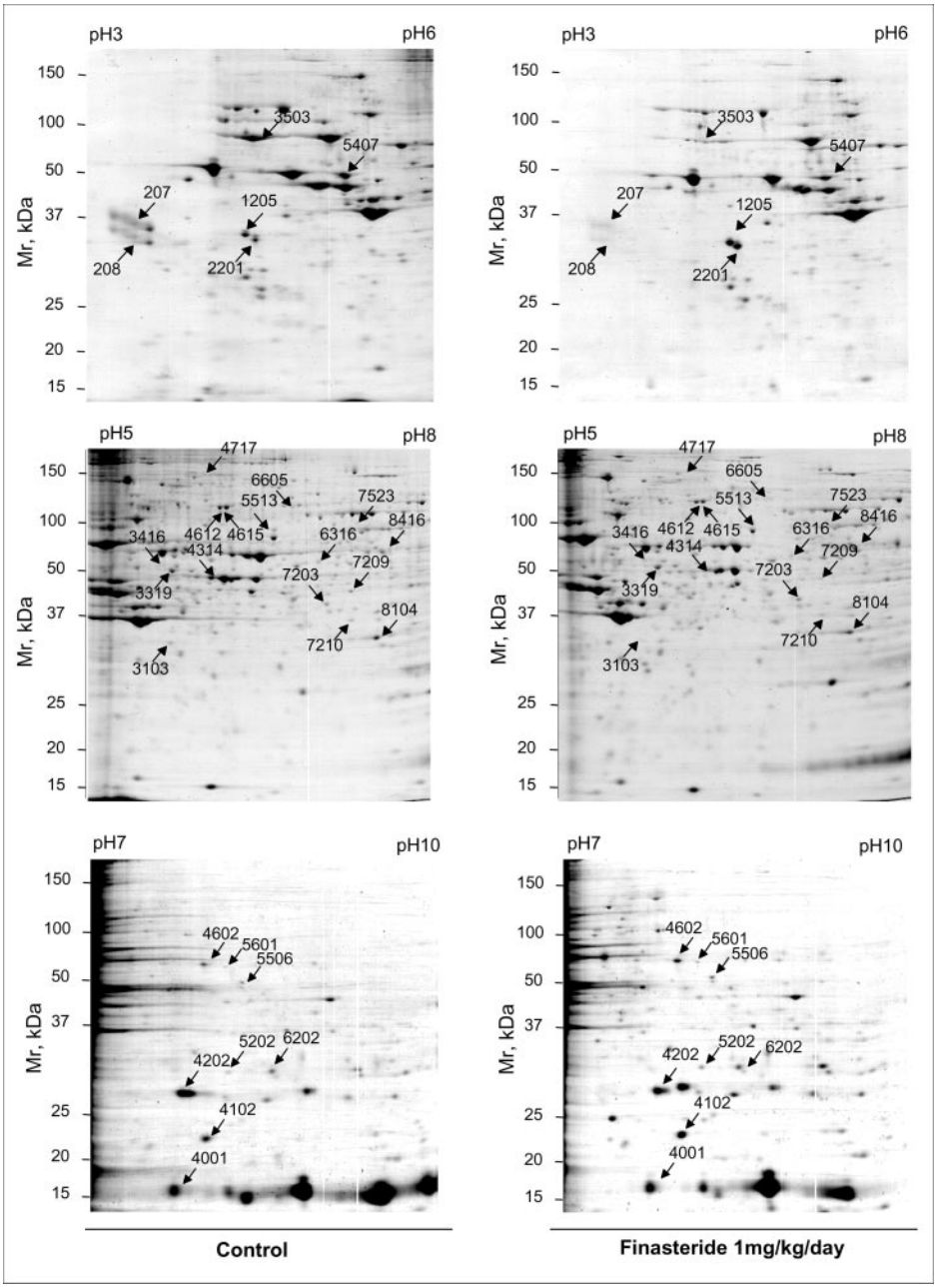

FIG. 3. **2D-gel pattern of control and finasteride-treated rats (1 mg/kg/day).** 500 μg of rat ventral prostate proteins were first separated by IEF on different immobilized pH gradients (pH 3–6, pH 5–8, and pH 7–10) and then by SDS-PAGE (10% acrylamide). Spots were visualized by Coomassie Blue staining. Representative 2D-gels from control and finasteride-treated (1 mg/kg/day) rats are presented. *Numbered spots* correspond to proteins exhibiting a modified expression level upon finasteride treatment (details on identifications are presented in Tables II and III).

are indicated with an *arrow* and an *identification number* as allocated by PD-Quest software. Image analysis of electrophoretic patterns revealed that finasteride significantly modified the expression of 40 spots among which 37 were identified by mass spectrometry (MALDI-TOF and/or ESI-MS/MS). Spot identities, MOWSE (molecular weight search) scores, mean normalized intensity ratios of treated *versus* control rats, statistical parameters, and reference articles related to the genes already shown to be androgen-regulated are presented in Table II. Unidentified proteins are presented in Table III.

The identified proteins have roughly been classified in six groups according to their functions. The first group corresponds to 11 proteins, down-regulated in response to finasteride treatment, that are involved in protein synthesis, processing, and cellular trafficking: EeF1γ (transcription factor), aspartyl- and arginyl-tRNA synthase (polypeptide synthesis), α-mannosidase 2C1 and sialic acid synthase (post-translational modifications), a protein similar to coat protein γ-COP, two forms of β-COP subunits and clathrin (vesicular transport and secretion), and three secreted proteins (two forms of prostatic spermine-binding protein, which have been described to differ by their degree of glycosylation (24); a cystatin-related protein; and S3 glandular kallikrein).

The second group includes proteins involved in cellular

TABLE II

Putative proteins modulated by finasteride treatment in rat ventral prostate identified by mass spectrometry

Shown are sample spot protein numbers of statistically regulated spots as assessed by PD-Quest 7.1 image analysis software, score, name and sequence accession number obtained from Swiss-Prot or nrNCBI databases, ratios of treated *versus* control for finasteride at 1 (R1), 5 (R5), 25 (R25), and 125 (R125) mg/kg/day.

Spot number	Score	Protein coverage	Protein name	Accession number	R1	R5	R25	R125	Related articles
Proteins involved in synthesis, processing, and cellular trafficking–Secreted proteins									
		%							
7203	2.5e+4	32	Eukaryotic translation elongation factor 1γ	34856454	0.52[a]	0.55[a]	0.33[b]	0.32[a]	15
6316	1.e+7	38	Aspartyl-tRNA synthetase	P15178	0.39[b]	0.28[b]	0.34[b]	0.01[a]	16
8416	6.4e+6	45	Similar to arginyl-tRNA synthetase	34870648	0.30[b]	0.65	0.16[a]	0.15[a]	16
6605	3.2e+5	12	α-Mannosidase 2C1	P21139	0.71	0.35[b]	0.44	1.3	
8104	4.1e+4	36	Similar to *N*-acetylneuraminic acid synthase	27714479	0.58[a]	0.5[a]	0.42[a]	0.20[a]	15
3501	2.6e+8	25	Similar to coat protein γ-COP	34856387	0.01[a]	0.25[a]	0.26[a]	0[a]	16
4612	8.5e+4	13	Coatomer β subunit	P23514	3.1[a]	0.01[a]	0.03[a]	0.01[a]	
4615	1.9e+13	39	Coatomer β subunit	P23514	3.1[a]	0.06[a]	0[a]	0[a]	
4717	1.2e+11	21	Clathrin heavy chain	P11442	0[a]	0.18[a]	0.03[a]	0.06[a]	33
207	1.1e+4	19	Prostatic spermine-binding protein (precursor)	P08723	0.93	0.54	0.28[b]	0.42	49
208	2.5e+3	15	Prostatic spermine-binding protein (precursor)	P08723	0.98	0.58	0.28[b]	0.43	49
4001	35.1[c]	25	Cystatin-related protein 1 precursor	P22282	0.44[b]	0.35[b]	0.83	0.39[a]	30
4202	1.1e+3	22	Glandular kallikrein 9 (S3 kallikrein)	P07647	0.60	0.58	0.70	0.47[b]	50
Proteins involved in metabolism									
9103	5e+8	29	ATP synthase α chain, mitochondrial precursor	P15999	0.61[a]	0.53[b]	0.6[b]	0.7	
7401	7.5e+3	13	Fructose 6-phosphate 2-kinase/fructose-2,6-bisphosphatase	Q9JJH5	0.74	0.28[a]	0.54[b]	0.22[a]	
3103	8.2e+4	30	Farnesyl diphosphate synthase	P05369	0.3[a]	0.9	0.2[a]	0.08[a]	32
6404	2e+5	65	Fructose-bisphosphate aldolase A	P05065	1	1.13	1.54[b]	2.08[b]	
6202	4.7e+3	22	GAPDH	27715161	1.16	2.84[a]	1.43	1.64[b]	42
5506	9.1e+7	29	Pyruvate kinase, isozymes M1/M2	P11980	1.31	4.60[a]	0.02[a]	1.43	
4602	1.1e+11	33	Transketolase	P50137	1.96[b]	2.43[a]	1.91	1.33	
Proteins involved in cell morphology									
5513	1.6e+5	33	Ezrin	17902245	0.28[b]	0.22[b]	0.28[b]	0.21	16
5202	2.8e+6	47	Annexin II	Q07936	1.7[b]	3.38[a]	2.18[b]	2.39[a]	51
5407	2.3e+6	21	Similar to tubulin, α6	34868254	1.64[a]	1.54	1.69[a]	1.5[b]	17
2201	4.2e+3	34	Tropomyosin 1α isoform	P04692	1.88[b]	1.56	1.77	3.3[a]	
1205	6.8e+5	40	Tropomyosin β chain	P58775	2[a]	1.61	2.28[a]	3.38[a]	
Proteins involved in detoxication									
7209	2.7e+7	30	Aldehyde dehydrogenase, mitochondrial	P11884	0.04[a]	0.27[a]	0.12[b]	0.13[a]	
7210	2e+4	23	Aldehyde dehydrogenase 1A1	P51647	0.27[b]	0.38[b]	0.22[b]	0.15[a]	15
4102	1e+5	46	Glutathione *S*-transferase Yb-2	P08010	1.49	2.12[a]	1.61[b]	1.73[b]	52
Proteins related to oxidative stress									
3503	8.8e+7	25	78-kDa glucose-regulated protein [precursor]	P06761	0.71[a]	0.91	0.93	0.92	17
4314	5.2e+16	54	Disulfide isomerase A3	P11598	0.11[b]	0.46	0.28[b]	0.37[b]	17
3319	9.5e+3	20	60-kDa heat shock protein, mitochondrial precursor	16741093	1.59[b]	0.4	1.1	1.45	
2803	6.5e+4	19	Heat shock 70-related protein APG-2	Q61316	49[a]	62[a]	73[a]	76[b]	41
3416	7.1e+6	22	Similar to heat shock cognate 71-kDa protein	27684119	63.9[a]	7.9[a]	15.3[b]	183.9[b]	41
1701	8.9e+12	44	Heat shock protein HSP 90-β	P34058	2.4	1.28	3.03[a]	3.22[b]	17
8602	1.1e+14[c]	50	Similar to L-amino-acid oxidase 1	34870868	10.09[a]	13.44[a]	19.13[a]	14.37[a]	
Proteins related to apoptosis									
5601	1.2e+7	23	Programmed cell death protein 8, mitochondrial precursor	Q9JM53	1.88[b]	2.95[a]	0.07[a]	0.84	
701	9.1e+6	28	Similar to programmed cell death 6-interacting protein	34866400	5.7[a]	1.89	0[b]	2.59[a]	

[a] $p < 0.01$.
[b] $p < 0.05$.
[c] Identification confirmed by ESI-MS/MS.

metabolism. Three proteins were down-regulated due to finasteride exposure (ATP synthase α chain, an enzyme of the mitochondrial respiratory chain; farnesyl diphosphate synthase, an enzyme required for cholesterol biosynthesis as well as protein prenylation; and fructose 6-phosphate 2-kinase/fructose-2,6-bisphosphatase, a modulator of glycolytic fluxes in extrahepatic tissues). Four proteins were up-regulated following finasteride treatment (three glycolytic enzymes, fruc-

TABLE III

Unidentified proteins modulated by finasteride treatment in rat ventral prostate

Shown are sample spot protein numbers of statistically significant regulated spots as assessed by PD-Quest 7.1 image analysis software, score, sequence accession number obtained from nrNCBI databases, ratios of treated *versus* control for finasteride at 1 (R1), 5 (R5), 25 (R25), and 125 (R125) mg/kg/day.

Spot number	Score	Protein coverage	Accession number		R1	R5	R25	R125
		%						
2807	6.44*e*+14	37	Unknown (protein for MGC:91679)	47939011	2.12[a]	2.32[a]	2.59[a]	0.59
7508	1.5*e*+5	21	Similar to RIKEN cDNA 1810074P20	34867100	0.48[b]	0.67[b]	0.41[a]	0.75
7523	1.5*e*+4	18	Similar to RIKEN cDNA 1810074P20	34867100	0.48[a]	0.57[b]	0.41[a]	0.71

[a] $p < 0.05$.
[b] $p < 0.01$.

tose-bisphosphate aldolase A, glyceraldehyde-3-phosphate dehydrogenase, and pyruvate kinase; and transketolase, an enzyme involved in interconnection of glycolytic and pentose monophosphate shunt pathways).

The inhibition of DHT synthesis due to the inhibition of 5αR also resulted in the modulation of proteins involved in cell morphology and muscle contraction. Only ezrin, a protein that anchors actin to the plasma membrane, was down-regulated. Annexin II (a calcium-dependent, phospholipid- and membrane-binding protein), tubulin-α6 chain (a major constituent of microtubules), and tropomyosins 1α and 2β (muscle proteins of the I-band that inhibit contraction by blocking the interaction of actin and myosin) were up-regulated. Detoxification proteins were also affected by finasteride treatment, leading to a down-regulation of two aldehyde dehydrogenases (mitochondrial and cytosolic) and an up-regulation of glutathione *S*-transferase Yb-2.

A fifth group of proteins (mainly chaperones), related to oxidative stress, was also modulated. Two proteins located in endoplasmic reticulum, GRP 78 and disulfide isomerase A3, were down-regulated. All others in this group were up-regulated: heat shock protein (HSP) 60 (mitochondria), HSP 70-related protein APG-2, similar to heat shock cognate 71-kDa protein, and HSP 90-β (cytoplasm). Finally we found a multiphasic response for two proteins related to apoptosis: the mitochondrial precursor of the programmed cell death protein 8 and a protein similar to programmed cell death 6-interacting protein.

When expressed as the ratio treated/control (Table II), most of the observed variations appeared to be of low magnitude as already described for messenger RNA levels (Table II, see related references) with the exception of some proteins that were barely detectable either in control or stimulated conditions (possibly leading to overestimated treated/control ratios). Moreover some proteins exhibited an aberrant behavior characterized by consistent biphasic (*i.e.* β-COP) or even multiphasic responses (*i.e.* similar to programmed cell death-interacting protein). Such a behavior has already been observed for a well known androgen-regulated gene, prostatein C3, and still remains unexplained (2).

Finasteride Induces an Up-regulation of a Protein Similar to Lao1—An interesting effect of finasteride on the rat VP proteome was the significant up-regulation of a putative pro-oxidant protein similar to Lao1. Lao1 was detectable on the 2D-gels in basal conditions, although this protein was only weakly expressed (Fig. 4*A*). Under finasteride treatment, an up-regulation by 10-fold was observed at 1 mg/kg/day finasteride (in comparison with control value, $p < 0.01$) and by 19-fold at 25 mg/kg/day ($p < 0.01$). At the highest dose of finasteride, the increase in expression of Lao1 was slightly less pronounced (14-fold, $p < 0.01$), but this might reflect the deleterious effects of finasteride on the prostate tissue at this dose (Fig. 4, *A* and *B*).

Such an induction was also obtained with flutamide, a competitive inhibitor of AR (Fig. 4*C*). The induction profile was comparable to that observed with finasteride, namely an up-regulation at 6 and 30 mg/kg/day (3- and 9-fold increase, respectively) and a less pronounced effect at the highest dose tested (150 mg/kg/day, 6-fold increase). It is noteworthy that at the highest dose we observed an even more deleterious effect on hormonal levels for flutamide than for finasteride (see Supplemental Fig. 1S) and prostate tissue (see Supplemental Table IS and Supplemental Fig. 2S).

A kinetic study (Fig. 4*D*) revealed that a 14-fold increase in Lao1 expression could be observed as soon as 48 h after the administration of a single bolus (150 mg/kg) of flutamide. No effect could be detected at 24 h (data not shown).

Immunolocalization of Lao1-like Protein—To identify the nature of the cells expressing Lao1, VP sections of control and finasteride-treated rats (25 mg/kg/day) were labeled with a polyclonal antibody, which was raised against snake venom Lao (the only commercially available anti-Lao antibody). Prior to this treatment, the antibody was first evaluated by Western blot to determine its ability to recognize rat Lao1 as shown in Fig. 5*A*.

Immunohistochemistry was subsequently performed using the Lao antibody on control and finasteride-treated VP sections (Fig. 5*B*). Microscopic examination of control sections revealed a faint Lao1 expression restricted to the perinucleolar area facing the apical pole and to membrane-bound secretory vesicles of the epithelium. Finasteride led to an enhanced labeling of these epithelial compartments. In addition, Lao1 labeling was no longer restricted to foci as in controls

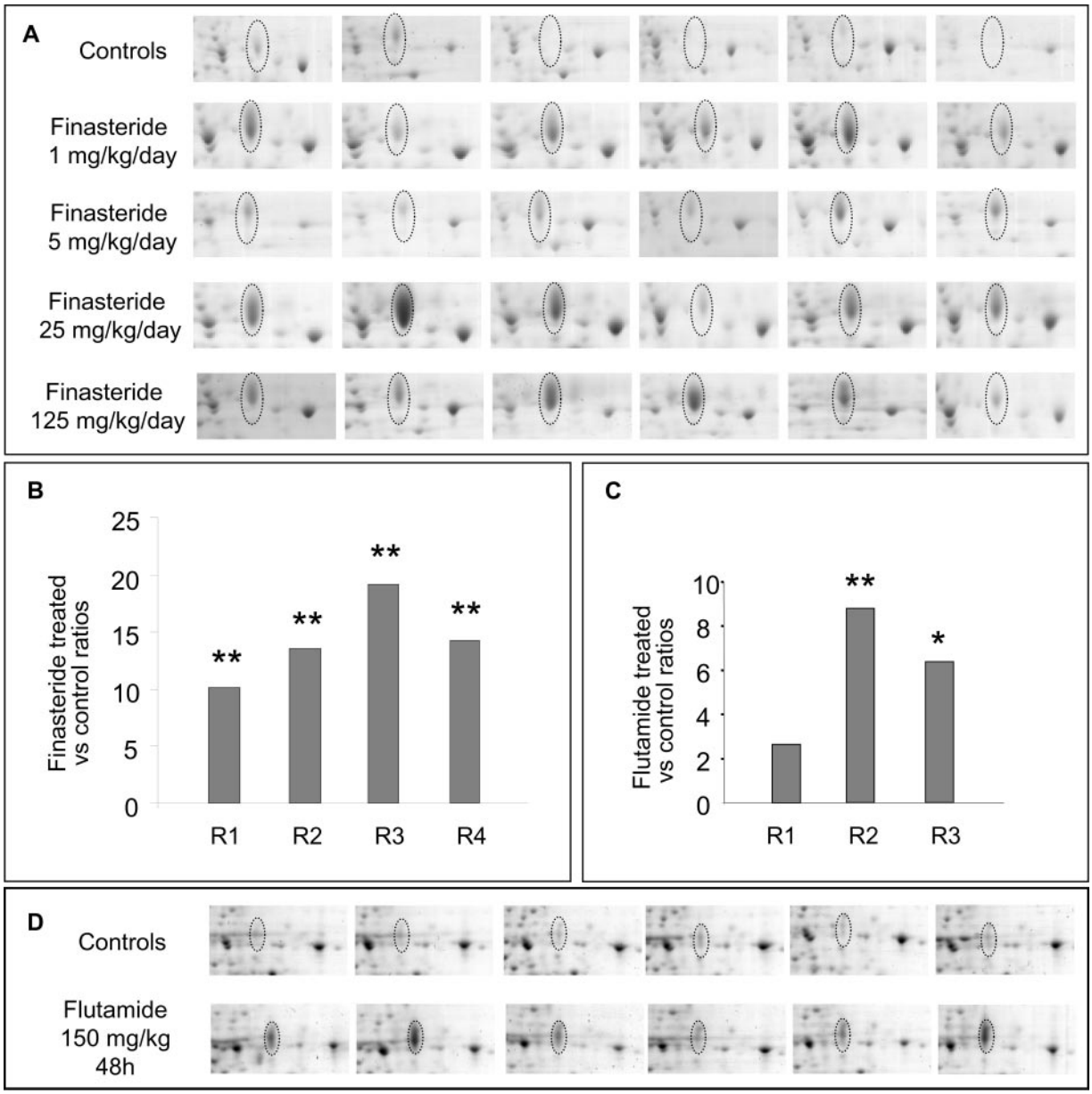

FIG. 4. **L-Amino-acid oxidase profile and intensity in control and finasteride- or flutamide-treated animals.** *A*, sections of individual 2D-gels (pH 3–10) from all control and 28-day finasteride-treated animals. *Dashed circles* indicate the position of Lao1. *B*, histogram of 28-day finasteride-treated *versus* control ratios of mean Lao1 intensities normalized with PD-Quest software (see "Experimental Procedures"). *R1*, *R2*, *R3*, and *R4*, groups treated at 1, 5, 25, and 125 mg/kg/day, respectively. **, statistically different from control value ($p < 0.01$). *C*, histogram of 28-day flutamide-treated *versus* control ratios of mean Lao1 intensities normalized with PD-Quest software (see "Experimental Procedures"). *R1*, *R2*, and *R3*, groups treated at 6, 30, and 150 mg/kg/day, respectively. *Asterisks*, statistically different from control value (*, $p < 0.05$; **, $p < 0.01$). *D*, sections of individual 2D-gels (pH 3–10) from control and 48-h flutamide-treated animals. *Dashed circles* indicate the position of Lao1.

but was instead spread throughout the entire epithelium layer.

Effect of Finasteride on Protein Tyrosine Phosphorylation—Lao has been shown to oxidize amino acids and produce hydrogen peroxide (25), a reactive oxygen species known to increase protein tyrosine phosphorylation through the inhibition of protein tyrosine phosphatases (26, 27). To assess whether the up-regulation of Lao1 induced by finasteride came with an increase in protein tyrosine phosphorylation, rat ventral prostate proteins were blotted and incubated with anti-phosphotyrosine antibodies. As shown on Fig. 6*A2*, protein tyrosine phosphorylation in the RH-soluble fraction increased (up to 75% above the basal value) in a dose-dependent manner with finasteride concentration. Phosphoproteins with molecular masses ranging from 25 to 130 kDa were roughly affected to the same extent. The pattern obtained with the RH-insoluble material (Fig. 6*B2*) was different with an

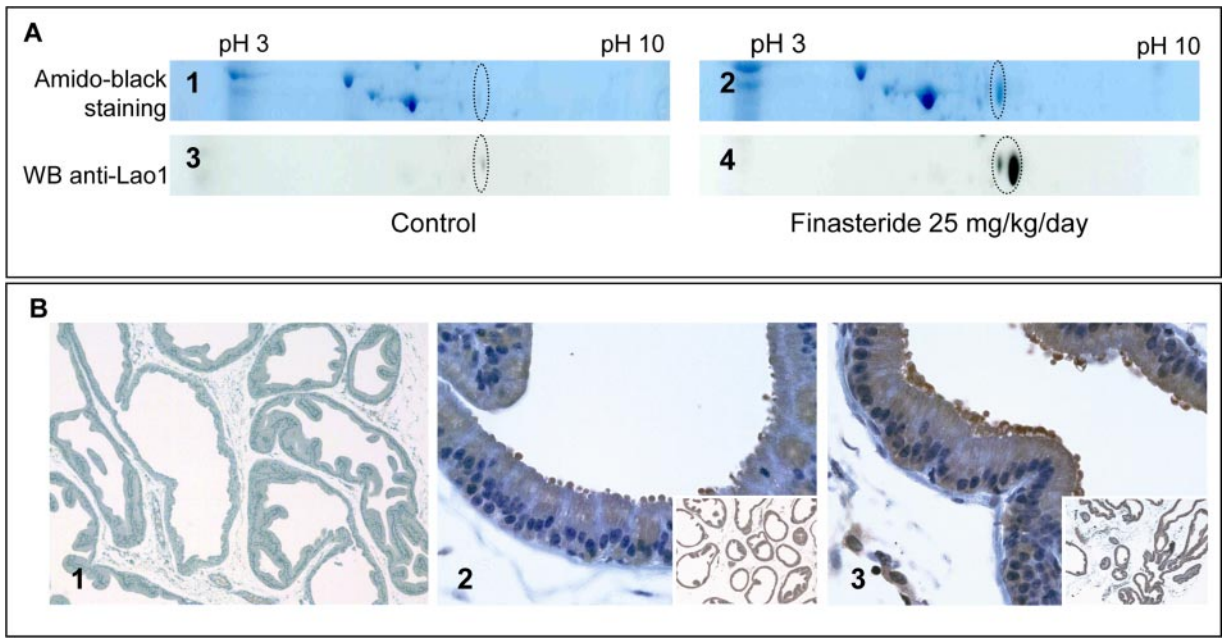

FIG. 5. **Western blot and immunolocalization of L-amino-acid oxidase in ventral prostate tissue of control and treated rats.** *A*, proteins of VP from control and treated rats were electrophoretically transferred from 2D-gels to PVDF membranes. *1* and *2*, PVDF membranes stained with Amido Black (see "Experimental Procedures"). *3* and *4*, autoradiograms of Western blots (*WB*) hybridized with Lao antibody. *B*, immunostaining of VP sections of control and finasteride (25 mg/kg/day)-treated animals. *1*, nonimmune staining (×100); *2* and *3*, Lao1 staining of control and treated rats, respectively (×400; *inset*, ×50).

increased tyrosine phosphorylation occurring mainly on high molecular mass proteins (80–170 kDa) as observed at 25 and 125 mg/kg/day (15 and 72%, respectively).

DISCUSSION

Consistent with the 28-day study of Shao *et al.* (2), treatment of young adult male rats with finasteride produced a dramatic decrease in VP weight. A significant reduction in seminal vesicle, epididymis, and Cowper gland weights was also observed as these organs are also partially dependent on DHT for their homeostasis (28). The VP weight loss was the consequence of a marked atrophy of the tissue (10, 11, 29), a phenomenon constantly associated to finasteride treatment, and a decrease of epithelial cell proliferation. No effect of caspase-3 cleavage, analyzed by immunoblotting (data not shown), could be detected indicating that at 28 days apoptosis is no longer responsible for prostate atrophy. This is in agreement with a previous study performed by Rittmaster *et al.* (11) that showed that apoptotic events induced by finasteride occurred in a window ranging from day 4 to day 14.

Prahalada *et al.* (9) showed that exposure to finasteride (160 mg/kg/day) for 15 days induced a not statistically significant up-regulation of plasma T level. In our model the increase of serum T level at day 28 of finasteride treatment (125 mg/kg/day) was statistically significant. The level of LH remained unchanged in our study and therefore could not account for the T up-regulation; it is likely that the increase in T level resulted from an accumulation of this hormone due to 5αR inhibition.

Similar results were obtained with flutamide except that this antiandrogen had a more deleterious effect on the organ, characterized by more important weight loss and tissue structure shrinkage at the highest dose tested. Unlike finasteride, flutamide increased LH plasma level in a dose-dependent manner.

Changes in hormone levels, weight, and histology of sex accessory tissues are standard parameters for evaluating the action of androgenic or antiandrogenic compounds in male rodents. Recent studies have suggested that the use of more sensitive methods, such as microarray analyses, are necessary to unravel the mode of action of these agents (17). To address this problem, we made use of the proteomics approach to investigate the mechanisms involved in VP atrophy following exposure of rats to finasteride. Despite a significant weight loss in VP, the protein profiles were well preserved across the various concentrations of finasteride tested. This is consistent with previous morphometric analyses, which showed that following finasteride treatment stromal and glandular tissues were affected to the same extent in rat VP, leaving the volume ratio between these tissues unmodified (9). It is worth mentioning that most of the effects on protein expression were observed from the lowest dose of finasteride even in animals exhibiting no VP atrophy (that is four of six animals, Fig. 2). This suggests that these effects are more likely due to DHT deprivation than to secondary effects of prostate atrophy.

Androgens have been described as being able to regulate

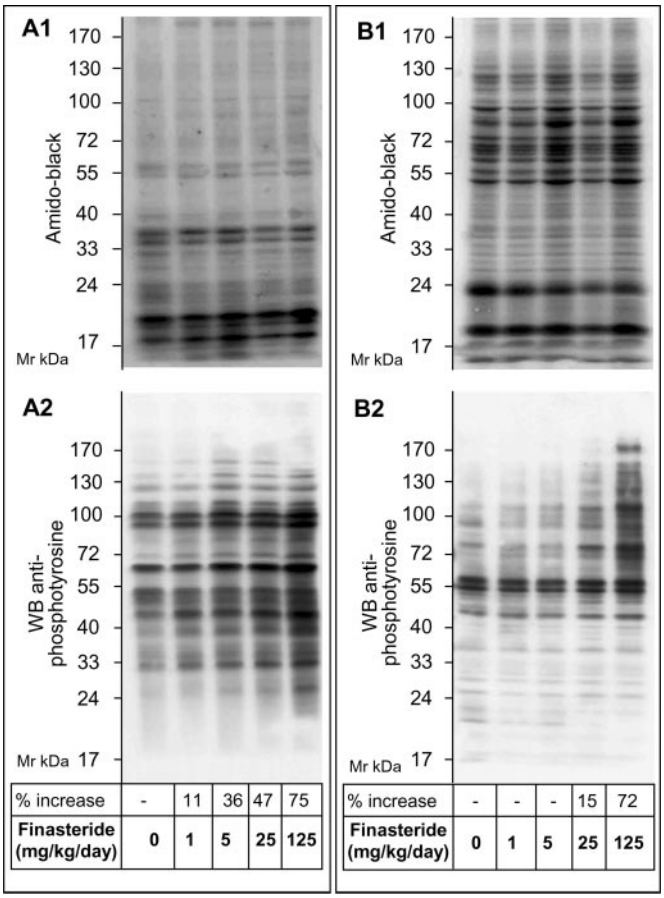

FIG. 6. **Effects of finasteride on protein tyrosine phosphorylation.** Protein extracts, within each group of six animals, were pooled and layered (75 μg/lane) on the top of a polyacrylamide gel (5–15%). After electrophoresis proteins were transferred onto PVDF membranes, stained with Amido Black, and then incubated with monoclonal anti-phosphotyrosine antibodies. *A1* and *B1*, Amido Black pattern of RH-soluble and -insoluble fractions, respectively. *A2* and *B2*, protein tyrosine phosphorylation profile of RH-soluble and -insoluble fractions, respectively. *WB*, Western blot.

prostatic secretory functions as well as the expression of secreted proteins (15, 24, 30). In this regard we observed under DHT withdrawal a down-regulation of enzymes involved in protein glycosylation pathways (α-mannosidase 2C1 and sialic acid synthase (31) and farnesyl diphosphate synthase (32)), of proteins involved in vesicular transport and secretion (clathrin (33), a protein similar to γ-COP, and two forms of β-COP subunits (16)), and of secreted proteins (prostatic binding protein, cystatin-related protein, kallikreins, and prostatic spermine-binding protein). Kallikrein S3 has been related to human prostate-specific antigen (34).

Several groups have proposed that one of the earliest changes leading to VP shrinking following castration or finasteride treatment is a decrease of prostate vascularization (35, 36), which induces hypoxia, and an associated up-regulation of a typical hypoxic transcription factor, hypoxia-inducible factor-1α (37). Aldolase A, glyceraldehyde-3-phosphate dehydrogenase, and pyruvate kinase M were up-regulated upon finasteride treatment. These glycolytic enzymes have been shown to be up-regulated by hypoxia-inducible factor-1α (38). Hypoxia can also down-regulate the respiratory and metabolic activities of mitochondria: this could explain the decrease of mitochondrial aldehyde dehydrogenase and ATP synthase α chain expression.

In addition, HSP up-regulation in exposure to hypoxia has been well described in the heart, especially HSP 60 and HSP 70 chaperone families, which are involved in cellular protection (39). HSPs can also act as important modulators of apoptotic cell death (40). We observed a consistent up-regulation of different chaperones (mitochondrial HSP 60, a protein similar to heat shock cognate 71-kDa protein, heat shock 70-related protein APG-2 and HSP 90-β) in our study. The induction of HSP 70-related genes has already been described in VP following castration (41). The up-regulation of HSP 90 and the down-regulations of GRP 78 and disulfide isomerase A3 in our study are in agreement with a previous study of Rosen *et al.* (17).

GAPDH was also up-regulated due to DHT deprivation in the present study. Epner *et al.* (42) showed that GAPDH was up-regulated in rat VP epithelial cells and translocated to the nuclei following castration, raising the possibility that GAPDH could also play a role in DNA repair in addition to its role in glycolysis within the cytoplasm.

Nevertheless taken together all the above mentioned changes were of a rather modest amplitude. This is in contrast with the huge increase in the expression of a protein similar to Lao1 that we observed in the VP tissue administered with finasteride. To ascertain whether Lao1 expression was related to the VP tissue damages, we used an antiandrogen, flutamide. This drug mediates its effects via a different mechanism than finasteride by inhibiting the binding of DHT or testosterone on the AR. Interestingly the expression of Lao1 was also dramatically increased in VP tissue after flutamide treatment.

Lao is a member of the flavoenzymes, which transform L-amino acids into their corresponding α-keto acids with the concomitant release of hydrogen peroxide and ammonia. Lao is widely distributed in various organisms (bacterial, fungal, plant, snake, and mammalian species) with the snake venom enzyme being by far the best documented (25). Lao can induce cell death by apoptosis through H_2O_2-dependent and/or -independent pathways involving amino acid depletion (43, 44). Two new Lao family members were recently identified in mammalians: the interleukin-4-induced gene-1 isolated in mouse leukocytes (45) and a mouse milk Lao1 (46). They share a 41.4% identity and a 80.7% identity, respectively, with the rat Lao1 that we identified in rat VP. The latter presents a conserved key domain and residues involved in the binding of the FAD cofactor required for enzymatic activity.

Interestingly Tam *et al.* (47) have shown recently that androgen deprivation in castrated rats clearly induces oxidative

stress in the regressing prostate epithelium and that testosterone replacement partially reduces this oxidative stress. The dramatic increase in Lao1 observed both in the cellular compartment and secretory vesicles from prostate epithelial cells of antiandrogen-treated rats could lead to oxidative stress through an overproduction of H_2O_2. This reactive oxygen species has been reported to increase the global pattern of cellular tyrosine phosphorylation by inhibiting the activity of protein tyrosine phosphatases (26, 27). Because it was virtually impossible to measure H_2O_2 content in frozen VP tissue we thought it was of interest to use the level of tyrosine phosphorylation as an indirect reporter of H_2O_2 production. Finasteride treatment actually resulted in a dose-dependent increase of protein tyrosine phosphorylation both in RH-soluble and -insoluble fractions.

As shown in B cells by Takano *et al.* (48), oxidative stress induces the activation of multiple signaling pathways related to various cellular responses such as mitotic arrest, apoptosis, and necrosis, depending on the H_2O_2 concentrations. This might explain the aggravation of prostate tissue injury upon exposure to increasing doses of antiandrogen, a phenomenon that could be linked to overexpression of Lao1 and a subsequent enzymatic H_2O_2 production. In addition, we showed a decrease in VP epithelial cell proliferation under finasteride treatment that also could be a consequence of H_2O_2 accumulation.

In conclusion, the current proteome analysis of VP from finasteride-treated rats revealed an altered expression of an array of proteins reflecting an impairment of epithelial cell secretory functions and disruption of oxidative stress, detoxification, and apoptosis, which could be at least partially responsible for the prostatic atrophy observed following treatment. The prominent feature of this study remains the demonstration of the dose-dependent up-regulation of a protein similar to Lao1. The fact that this protein was increased in VP tissue as soon as 48 h after flutamide administration lends support to the notion that Lao1 could be considered as an early marker of antiandrogenic action on VP tissue.

Acknowledgment—We thank Aline Lorefice for valuable help for the immunohistochemistry on rat VP.

* This work was supported in part by INSERM and Bayer CropScience. The costs of publication of this article were defrayed in part by the payment of page charges. This article must therefore be hereby marked "*advertisement*" in accordance with 18 U.S.C. Section 1734 solely to indicate this fact.

S The on-line version of this article (available at http://www.mcponline.org) contains supplemental material.

¶ Recipient of a fellowship co-sponsored by the French Ministry of Research and Bayer CropScience.

** To whom correspondence should be addressed. Tel.: 33-4-93-37-77-04; Fax: 33-4-93-81-94-56; E-mail: samson@unice.fr.

REFERENCES

1. Debes, J. D., and Tindall, D. J. (2002) The role of androgens and the androgen receptor in prostate cancer. *Cancer Lett.* **187,** 1–7
2. Shao, T. C., Kong, A., Marafelia, P., and Cunningham, G. R. (1993) Effects of finasteride on the rat ventral prostate. *J. Androl.* **14,** 79–86
3. Kelce, W. R., Gray, L. E., and Wilson, E. M. (1998) Antiandrogens as environmental endocrine disruptors. *Reprod. Fertil. Dev.* **10,** 105–111
4. Swan, S. H., Kruse, R. L., Liu, F., Barr, D. B., Drobnis, E. Z., Redmon, J. B., Wang, C., Brazil, C., and Overstreet, J. W. (2003) Semen quality in relation to biomarkers of pesticide exposure. *Environ. Health Perspect.* **111,** 1478–1484
5. Sultan, C., Balaguer, P., Terouanne, B., Georget, V., Paris, F., Jeandel, C., Lumbroso, S., and Nicolas, J. (2001) Environmental xenoestrogens, antiandrogens and disorders of male sexual differentiation. *Mol. Cell. Endocrinol.* **178,** 99–105
6. Rittmaster, R. S. (1994) Finasteride. *N. Engl. J. Med.* **330,** 120–125
7. Span, P. N., Voller, M. C., Smals, A. G., Sweep, F. G., Schalken, J. A., Feneley, M. R., and Kirby, R. S. (1999) Selectivity of finasteride as an in vivo inhibitor of 5α-reductase isozyme enzymatic activity in the human prostate. *J. Urol.* **161,** 332–337
8. Azzolina, B., Ellsworth, K., Andersson, S., Geissler, W., Bull, H. G., and Harris, G. S. (1997) Inhibition of rat α-reductases by finasteride: evidence for isozyme differences in the mechanism of inhibition. *J. Steroid Biochem. Mol. Biol.* **61,** 55–64
9. Prahalada, S., Rhodes, L., Grossman, S. J., Heggan, D., Keenan, K. P., Cukierski, M. A., Hoe, C. M., Berman, C., and van Zwieten, M. J. (1998) Morphological and hormonal changes in the ventral and dorsolateral prostatic lobes of rats treated with finasteride, a 5-α reductase inhibitor. *Prostate* **35,** 157–164
10. Prahalada, S. R., Keenan, K. P., Hertzog, P. R., Gordon, L. R., Peter, C. P., Soper, K. A., van Zwieten, M. J., and Bokelman, D. L. (1994) Qualitative and quantitative evaluation of prostatic histomorphology in rats following chronic treatment with finasteride, a 5-α reductase inhibitor. *Urology* **43,** 680–685
11. Rittmaster, R. S., Manning, A. P., Wright, A. S., Thomas, L. N., Whitefield, S., Norman, R. W., Lazier, C. B., and Rowden, G. (1995) Evidence for atrophy and apoptosis in the ventral prostate of rats given the 5α-reductase inhibitor finasteride. *Endocrinology* **136,** 741–748
12. Shibata, Y., Ono, Y., Kashiwagi, B., Suzuki, K., Fukabori, Y., Honma, S., and Yamanaka, H. (2003) Hormonal and morphologic evaluation of the effects of antiandrogens on the blood supply of the rat prostate. *Urology* **62,** 942–946
13. Kennel, P., Pallen, C., Barale-Thomas, E., Espuna, G., and Bars, R. (2003) Tamoxifen: 28-day oral toxicity study in the rat based on the Enhanced OECD Test Guideline 407 to detect endocrine effects. *Arch. Toxicol.* **77,** 487–499
14. Wason, S., Pohlmeyer-Esch, G., Pallen, C., Palazzi, X., Espuna, G., and Bars, R. (2003) 17α-Methyltestosterone: 28-day oral toxicity study in the rat based on the "Enhanced OECD Test Guideline 407" to detect endocrine effects. *Toxicology* **192,** 119–137
15. Jiang, F., and Wang, Z. (2003) Identification of androgen-responsive genes in the rat ventral prostate by complementary deoxyribonucleic acid subtraction and microarray. *Endocrinology* **144,** 1257–1265
16. Pang, S. T., Dillner, K., Wu, X., Pousette, A., Norstedt, G., and Flores-Morales, A. (2002) Gene expression profiling of androgen deficiency predicts a pathway of prostate apoptosis that involves genes related to oxidative stress. *Endocrinology* **143,** 4897–4906
17. Rosen, M. B., Wilson, V. S., Schmid, J. E., and Gray, L. E. (2005) Gene expression analysis in the ventral prostate of rats exposed to vinclozolin or procymidone. *Reprod. Toxicol.* **19,** 367–379
18. Lottspeich, F. (1999) Proteome analysis: a pathway to the functional analysis of proteins. *Angew. Chem. Int. Ed. Engl.* **38,** 2476–2492
19. Goldspiel, B. R., and Kohler, D. R. (1990) Flutamide: an antiandrogen for advanced prostate cancer. *DICP Ann. Pharmacother.* **24,** 616–623
20. Laemmli, U. K. (1970) Cleavage of structural proteins during the assembly of the head of bacteriophage T4. *Nature* **227,** 680–685
21. Olsson, I., Larsson, K., Palmgren, R., and Bjellqvist, B. (2002) Organic disulfides as a means to generate streak-free two-dimensional maps with narrow range basic immobilized pH gradient strips as first dimension. *Proteomics* **2,** 1630–1632
22. Kopchick, J. J., List, E. O., Kohn, D. T., Keidan, G. M., Qiu, L., and Okada, S. (2002) Perspective: proteomics—see "spots" run. *Endocrinology* **143,** 1990–1994
23. Righetti, P. G., Castagna, A., Antonucci, F., Piubelli, C., Cecconi, D.,

Campostrini, N., Antonioli, P., Astner, H., and Hamdan, M. (2004) Critical survey of quantitative proteomics in two-dimensional electrophoretic approaches. *J. Chromatogr. A* **1051,** 3–17
24. Chang, C. S., Saltzman, A. G., Hiipakka, R. A., Huang, I. Y., and Liao, S. S. (1987) Prostatic spermine-binding protein. Cloning and nucleotide sequence of cDNA, amino acid sequence, and androgenic control of mRNA level. *J. Biol. Chem.* **262,** 2826–2831
25. Du, X. Y., and Clemetson, K. J. (2002) Snake venom L-amino acid oxidases. *Toxicon* **40,** 659–665
26. Hecht, D., and Zick, Y. (1992) Selective inhibition of protein tyrosine phosphatase activities by H_2O_2 and vanadate in vitro. *Biochem. Biophys. Res. Commun.* **188,** 773–779
27. Heffetz, D., Bushkin, I., Dror, R., and Zick, Y. (1990) The insulinomimetic agents H_2O_2 and vanadate stimulate protein tyrosine phosphorylation in intact cells. *J. Biol. Chem.* **265,** 2896–2902
28. Steers, W. D. (2001) 5α-Reductase activity in the prostate. *Urology* **58,** 17–24
29. Ruska, K. M., Sauvageot, J., and Epstein, J. I. (1998) Histology and cellular kinetics of prostatic atrophy. *Am. J. Surg. Pathol.* **22,** 1073–1077
30. Vercaeren, I., Vanaken, H., Devos, A., Peeters, B., Verhoeven, G., and Heyns, W. (1996) Androgens transcriptionally regulate the expression of cystatin-related protein and the C3 component of prostatic binding protein in rat ventral prostate and lacrimal gland. *Endocrinology* **137,** 4713–4720
31. Iusem, N. D., De Larminat, M. A., Tezon, J. G., Blaquier, J. A., and Belocopitow, E. (1984) Androgen dependence of protein N-glycosylation in rat epididymis. *Endocrinology* **114,** 1448–1453
32. Jiang, F., Yang, L., Cai, X., Cyriac, J., Shechter, I., and Wang, Z. (2001) Farnesyl diphosphate synthase is abundantly expressed and regulated by androgen in rat prostatic epithelial cells. *J. Steroid Biochem. Mol. Biol.* **78,** 123–130
33. Prescott, J. L., and Tindall, D. J. (1998) Clathrin gene expression is androgen regulated in the prostate. *Endocrinology* **139,** 2111–2119
34. Onozawa, M., Fukuda, K., Watanabe, M., Ohtani, M., Akaza, H., Sugimura, T., and Wakabayashi, K. (2001) Detection and cloning of a protein recognized by anti-human prostate-specific antigen (PSA) antibody in the rat ventral prostate. *Jpn. J. Cancer Res.* **92,** 863–868
35. Haggstrom, S., Torring, N., Moller, K., Jensen, E., Lund, L., Nielsen, J. E., Bergh, A., and Damber, J. E. (2002) Effects of finasteride on vascular endothelial growth factor. *Scand. J. Urol. Nephrol.* **36,** 182–187
36. Shabisgh, A., Tanji, N., D'Agati, V., Burchardt, M., Rubin, M., Goluboff, E. T., Heitjan, D., Kiss, A., and Buttyan, R. (1999) Early effects of castration on the vascular system of the rat ventral prostate gland. *Endocrinology* **140,** 1920–1926
37. Shabsigh, A., Ghafar, M. A., de la Taille, A., Burchardt, M., Kaplan, S. A., Anastasiadis, A. G., and Buttyan, R. (2001) Biomarker analysis demonstrates a hypoxic environment in the castrated rat ventral prostate gland. *J. Cell. Biochem.* **81,** 437–444
38. Semenza, G. L., Roth, P. H., Fang, H. M., and Wang, G. L. (1994) Transcriptional regulation of genes encoding glycolytic enzymes by hypoxia-inducible factor 1. *J. Biol. Chem.* **269,** 23757–23763
39. Hammerer-Lercher, A., Mair, J., Bonatti, J., Watzka, S. B., Puschendorf, B., and Dirnhofer, S. (2001) Hypoxia induces heat shock protein expression in human coronary artery bypass grafts. *Cardiovasc. Res.* **50,** 115–124
40. Garrido, C., Gurbuxani, S., Ravagnan, L., and Kroemer, G. (2001) Heat shock proteins: endogenous modulators of apoptotic cell death. *Biochem. Biophys. Res. Commun.* **286,** 433–442
41. Buttyan, R., Zakeri, Z., Lockshin, R., and Wolgemuth, D. (1988) Cascade induction of c-fos, c-myc, and heat shock 70K transcripts during regression of the rat ventral prostate gland. *Mol. Endocrinol.* **2,** 650–657
42. Epner, D. E., Sawa, A., and Isaacs, J. T. (1999) Glyceraldehyde-3-phosphate dehydrogenase expression during apoptosis and proliferation of rat ventral prostate. *Biol. Reprod.* **61,** 687–691
43. Torii, S., Naito, M., and Tsuruo, T. (1997) Apoxin I, a novel apoptosis-inducing factor with L-amino acid oxidase activity purified from Western diamondback rattlesnake venom. *J. Biol. Chem.* **272,** 9539–9542
44. Sun, L. K., Yoshii, Y., Hyodo, A., Tsurushima, H., Saito, A., Harakuni, T., Li, Y. P., Kariya, K., Nozaki, M., and Morine, N. (2003) Apoptotic effect in the glioma cells induced by specific protein extracted from Okinawa Habu (Trimeresurus flavoviridis) venom in relation to oxidative stress. *Toxicol. In Vitro* **17,** 169–177
45. Mason, J. M., Naidu, M. D., Barcia, M., Porti, D., Chavan, S. S., and Chu, C. C. (2004) IL-4-induced gene-1 is a leukocyte L-amino acid oxidase with an unusual acidic pH preference and lysosomal localization. *J. Immunol.* **173,** 4561–4567
46. Sun, Y., Nonobe, E., Kobayashi, Y., Kuraishi, T., Aoki, F., Yamamoto, K., and Sakai, S. (2002) Characterization and expression of L-amino acid oxidase of mouse milk. *J. Biol. Chem.* **277,** 19080–19086
47. Tam, N. N., Gao, Y., Leung, Y. K., and Ho, S. M. (2003) Androgenic regulation of oxidative stress in the rat prostate: involvement of NAD(P)H oxidases and antioxidant defense machinery during prostatic involution and regrowth. *Am. J. Pathol.* **163,** 2513–2522
48. Takano, T., Sada, K., and Yamamura, H. (2002) Role of protein-tyrosine kinase syk in oxidative stress signaling in B cells. *Antioxid. Redox. Signal.* **4,** 533–541
49. Hiipakka, R. A., Chen, C., Schilling, K., Oberhauser, A., Saltzman, A., and Liao, S. (1984) Immunochemical characterization of the androgen-dependent spermine-binding protein of the rat ventral prostate. *Biochem. J.* **218,** 563–571
50. Wolf, D. A., Schulz, P., and Fittler, F. (1992) Transcriptional regulation of prostate kallikrein-like genes by androgen. *Mol. Endocrinol.* **6,** 753–762
51. Smitherman, A. B., Mohler, J. L., Maygarden, S. J., and Ornstein, D. K. (2004) Expression of annexin I, II and VII proteins in androgen stimulated and recurrent prostate cancer. *J. Urol.* **171,** 916–920
52. Hoshikawa, Y., and Sairenji, T. (1996) Selective enhancement of expression of class-Mu glutathione S-transferase genes during involution of rat ventral prostate induced by androgen withdrawal. *Yonago Acta Med.* **39,** 151–154